Azimuthal anisotropy in the asymmetric collisions at the NICA energy range

Азимутальная анизотропия в асимметричных столкновениях в области энергии НИКА

P. Parfenov[a,b,1], *A. Taranenko*[a,b]

П.Е. Парфенов[a,b], *А.В. Тараненко*[b]

[a] Joint Institute for Nuclear Research, Dubna, Russia

[a] Объединенный Институт Ядерных Исследований, г. Дубна, Россия

[b] National Research Nuclear University MEPhI, Moscow, Russia

[b] Национальный Исследовательский Ядерный Университет МИФИ, г. Москва, Россия

В экспериментах по изучению ядро-ядерных столкновений на многоцелевом детекторе (MPD) на ускорительном комплексе NICA будет исследоваться фазовая диаграмма КХД материи при высоких плотностях барионов в режимах коллайдера ($\sqrt{s_{\rm NN}}$=4–11 GeV) и фиксированной мишени ($\sqrt{s_{\rm NN}}$=2.3–3.5 GeV). Анизотропные коллективные потоки частиц в ядро-ядерных столкновениях, дают важную информацию об уравнении состояния и транспортных свойствах сильно взаимодействующей материи. В данной работе мы изучаем анизотропные потоки протонов и их эффекты масштабирования как в асимметричных (Xe+W), так и в симметричных (Xe+Xe и Au+Au) столкновениях при энергии $\sqrt{s_{\rm NN}}$= 2,87 ГэВ, используя в качестве основы расчеты в рамках модели UrQMD.

The Multi-Purpose Detector (MPD) experiment at NICA accelerator complex will investigate the phase diagram of QCD matter at high net-baryon densities in collider ($\sqrt{s_{\rm NN}}$=4–11 GeV) and fixed-target ($\sqrt{s_{\rm NN}}$=2.3–3.5 GeV) modes. Anisotropic flow, as measured by the azimuthal anisotropy of final-state particles, provides crucial insights into the equation of state and transport properties of strongly interacting matter. In this study, we examine the anisotropic flow of protons and its scaling relations in both asymmetric (Xe+W) and symmetric (Xe+Xe and Au+Au) colliding systems at $\sqrt{s_{\rm NN}}$= 2.87 GeV, using the UrQMD model calculations as a basis.

PACS: 44.25.+f; 44.90.+c

Introduction

Beam energy scan (BES) programs with relativistic heavy ion collisions provide an opportunity to study the phases of QCD matter at different temperatures and baryon densities. The ongoing BES programs include: programs BES-I and BES-II of STAR experiment at RHIC for Au+Au collisions at $\sqrt{s_{\rm NN}}$=3–200 GeV [1–5]; the program of NA61/SHINE experiment

[1]E-mail: pparfenov@jinr.int

at SPS for different colliding systems from Be+Be to Pb+Pb at $\sqrt{s_{\rm NN}}$=5.1–17.3 GeV [6] and the program of the BM@N experiment at Nuclotron for different colliding systems at $\sqrt{s_{\rm NN}}$=2.4–3.5 GeV [7]. The forthcoming MPD experiment at NICA will further probe the high-baryon-density region of the phase diagram in collider (MPD-COL:$\sqrt{s_{\rm NN}}$=4–11 GeV) and fixed-target (MPD-FXT: $\sqrt{s_{\rm NN}}$=2.3–3.5 GeV) modes of operation [8–10]. Anisotropic flow characterizes the collective anisotropy of particle emission in the plane transverse to the beam direction. It is a key observable sensitive to the equation of state and transport properties of the strongly interacting matter created in the relativistic heavy-ion collisions. It can be quantified by the Fourier coefficients $v_{\rm n}$ of the azimuthal distribution of the particles produced in the collision [11]:

$$\frac{dN}{d\varphi} \propto 1 + 2\sum_{\rm n=1}^{\infty} v_{\rm n} \cos\left(n\left(\varphi - \Psi_{\rm n}\right)\right), \tag{1}$$

where n is the harmonic order, φ is the particle's azimuthal angle, and $\Psi_{\rm n}$ is the $n^{\rm th}$-order symmetry plane. The flow coefficient of order n is defined as $v_{\rm n} = \langle\cos\left(n\left(\varphi - \Psi_{\rm n}\right)\right)\rangle$, with the average taken over particles and events.
The MPD-FXT program will provide a unique opportunity to systematically study anisotropic flow using different collision systems, including asymmetric ones such as Xe+W. The goal of this work is to examine the initial spatial anisotropy of the overlapping zone of two colliding nuclei (eccentricity), the final anisotropic flow of protons and its scaling relations in both asymmetric (Xe+W) and symmetric (Xe+Xe and Au+Au) colliding systems at $\sqrt{s_{\rm NN}}$= 2.87 GeV, using the UrQMD model calculations as a basis.

Eccentricity and its fluctuation in heavy ion collisions

The initial-state spatial azimuthal anisotropy is characterized by eccentricity coefficients $\varepsilon_{\rm n}$, defined in analogy to the anisotropic flow coefficients $v_{\rm n}$ in momentum space [12]:

$$\varepsilon_{\rm n} = \frac{\sqrt{\langle r^n \cos(n\varphi)\rangle^2 + \langle r^n \sin(n\varphi)\rangle^2}}{\langle r^n\rangle}, \tag{2}$$

where n is the harmonic order, and r and φ are the radial and azimuthal coordinates of a participant nucleon in the initial overlap region. The angle brackets $\langle\cdots\rangle$ denote an average over nucleons in a single event.
To quantify eccentricity fluctuations, we employ two- and four-particle cumulants and define a relative fluctuation parameter $\sigma(\varepsilon_{\rm n})$ [13, 14]:

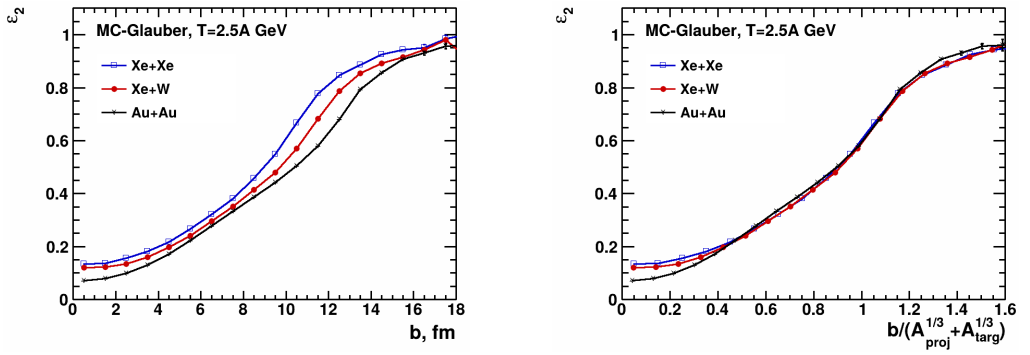
$$\varepsilon_{\rm n}\{2\} = \sqrt{\langle\varepsilon_{\rm n}^2\rangle}, \quad \varepsilon_{\rm n}\{4\} = \sqrt[4]{2\langle\varepsilon_{\rm n}^2\rangle^2 - \langle\varepsilon_{\rm n}^4\rangle}, \quad \sigma(\varepsilon_{\rm n}) = \frac{\varepsilon_{\rm n}\{4\}}{\varepsilon_{\rm n}\{2\}}. \tag{3}$$

Here, the angle brackets represent an average over events.
This work focuses on the second-order harmonic ($n = 2$), which is related to the second-order flow coefficient called elliptic flow v_2. In the following, the term "eccentricity" refers specifically to the second-harmonic eccentricity ε_2.

Results

This analysis employs 100k minimum-bias events generated with the Monte Carlo Glauber (MC-Glauber) [15] and UrQMD [16, 17] models at a beam kinetic energy of $T = 2.5$A GeV ($\sqrt{s_{\rm NN}} = 2.87$ GeV) for Xe+W, Xe+Xe, and Au+Au collision systems. The asymmetric Xe+W system represents the most probable scenario for the initial MPD-FXT run. The symmetric Xe+Xe and Au+Au systems provide reference baselines: Xe+Xe has a comparable overlap region size to Xe+W, while Au+Au serves as a standard benchmark used in the BES program of the STAR experiment.

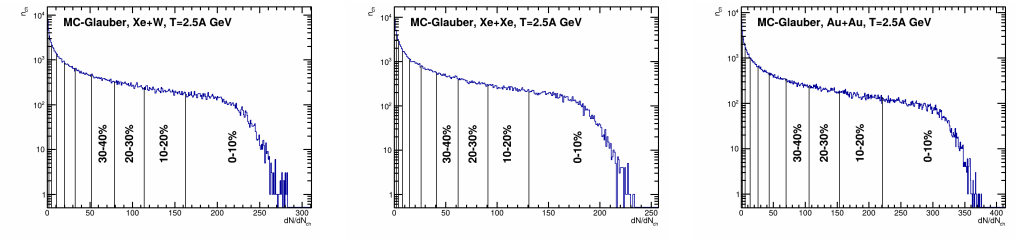
Figure 1(a) shows the eccentricity ε_2 as a function of the impact parameter b. To account for the system size, we define a scaled impact parameter as $b/(A_{\rm proj}^{1/3} + A_{\rm targ}^{1/3})$ where $A_{\rm proj}$ and $A_{\rm targ}$ are the atomic masses of the projectile and the target correspondingly. As shown in Fig. 1(b), this scaling effectively describes ε_2 across the different collision systems. For a more realistic study of the eccentricity and its fluctuations, we use charged-particle multiplicity $N_{\rm ch}$ as a proxy for the collision centrality. Since the MC-Glauber model does not generate final-state particles, $N_{\rm ch}$ is sampled using the Kharzeev-Nardi approach [18], where the number of "ancestors" is given by $N_{\rm a} = fN_{\rm part} + (1-f)N_{\rm coll}$, with $N_{\rm part}$ and $N_{\rm coll}$ are being the number of participant nucleons in the collision and corresponding binary nucleon-nucleon collisions, provided by the MC-Glauber model. Convolving $N_{\rm a}$ with a negative binomial distribution yields the $N_{\rm ch}$-distribution, which is then divided into uniform percentile centrality classes for subsequent analysis. The resulting multiplicity distributions and the defined centrality classes for each collision system are presented in Fig. 2.



(a) (b)

Fig. 1: Eccentricity ε_2 as a function of (a) impact parameter b and (b) scaled impact parameter $b/(A_{\rm proj}^{1/3} + A_{\rm targ}^{1/3})$ from the Monte Carlo Glauber model (MC-Glauber) for a beam kinetic energy of $T = 2.5A$ GeV. Results are shown for different collision systems: Xe+Xe (blue), Xe+W (red), and Au+Au (black).

Figures 3 and 4 present the eccentricity ε_2 and its relative fluctuation $\sigma(\varepsilon_2)$ as functions of centrality from the MC-Glauber (a) and UrQMD (b)

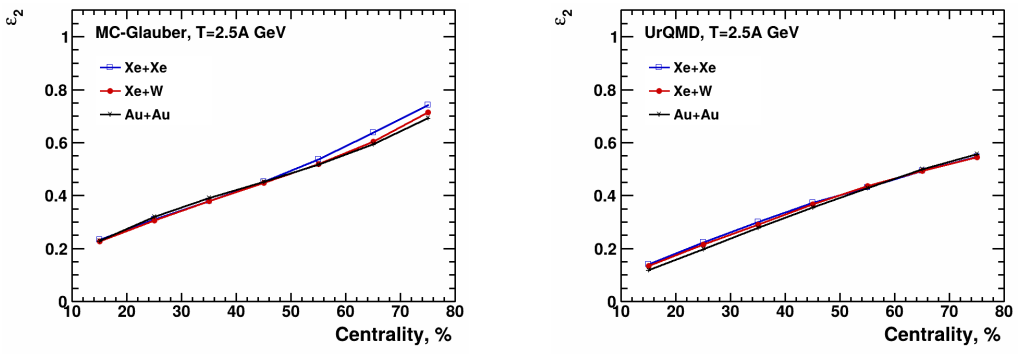


(a) (b) (c)

Fig. 2: Charged-particle multiplicity distributions, calculated via the Kharzeev-Nardi approach using $N_{\rm part}$ and $N_{\rm coll}$ from the MC-Glauber model, for three collision systems at a beam kinetic energy of $T = 2.5A$ GeV: (a) Xe+W, (b) Xe+Xe, and (c) Au+Au. Vertical lines indicate the multiplicity ranges used to define centrality classes for each system.

models. For the UrQMD calculation, ε_2 is defined using participant nucleons and produced particles existing within the passing time $t_{\rm pass}(b) = \sqrt{(R_{\rm targ} + R_{\rm proj})^2 - b^2}/\gamma_{\rm CM}\beta_{\rm CM}$, where R is the nuclear radius, b is the impact parameter, $\gamma_{\rm CM}$ and $\beta_{\rm CM}$ are the Lorentz factors in the center-of-mass (or rather center-of-velocity) frame. The MC-Glauber results indicate that while ε_2 scales with the system size and is similar across all three collision systems at a given centrality range, the relative fluctuation $\sigma(\varepsilon_2)$ differs significantly within the 10–60% centrality range. In contrast, UrQMD predicts similar scaling for both ε_2 and $\sigma(\varepsilon_2)$, suggesting that the large $t_{\rm pass}$ may allow fluctuations to subside, leading to more consistent values.

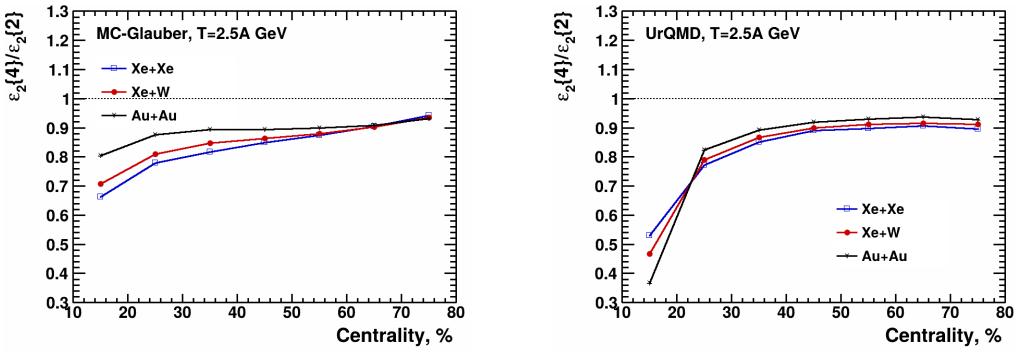
Figure 5 reveals a strong dependence of ε_2 and $\sigma(\varepsilon_2)$ on the collision evo-



(a) (b)

Fig. 3: Eccentricity as a function of collision centrality from (a) MC-Glauber and (b) UrQMD models at a beam kinetic energy of $T = 2.5A$ GeV. Results are shown for Xe+Xe (blue), Xe+W (red), and Au+Au (black) collisions. The UrQMD calculations incorporate nucleons and produced particles within the passing time $t_{\rm pass}$.

lution time. This underscores the need for a comprehensive strategy for a

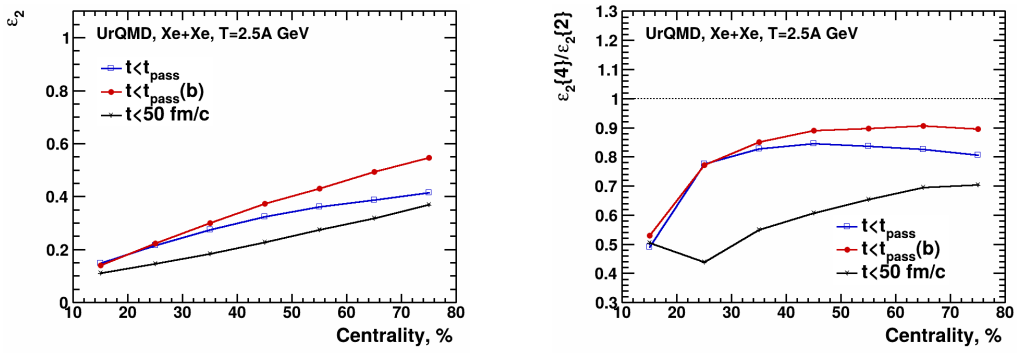


(a) (b)

Fig. 4: Relative eccentricity fluctuations as a function of collision centrality from (a) MC-Glauber and (b) UrQMD models at a beam kinetic energy of $T = 2.5A$ GeV. Results are shown for Xe+Xe (blue), Xe+W (red), and Au+Au (black) collisions. The UrQMD calculations incorporate nucleons and produced particles within the passing time $t_{\rm pass}$.

comparison of initial-state parameters between static (e.g., MC-Glauber) and dynamic (e.g., UrQMD) models, which remains a subject for the future investigation.

The observed differences in the relative eccentricity fluctuations may influ-



(a) (b)

Fig. 5: Eccentricity (a) and its relative fluctuation (b) as a function of collision centrality from the UrQMD model in Xe+Xe collisions at a beam kinetic energy of $T = 2.5A$ GeV. Different colors correspond to different evolution times. The blue lines represent the results taken at $t_{\rm pass} \equiv t_{\rm pass}(b = 0)$.

ence the development of the elliptic flow v_2. Figure 6(a) shows the proton v_2 as a function of transverse momentum $p_{\rm T}$ from 1M minimum-bias UrQMD events for each collision system at $T = 2.5$A GeV. Motivated by prior studies of v_2 scaling in the NICA energy range [19], we first have tested scaling by the integrated value $v_2^{\rm int}$ (Fig. 6(b)). This scaling unifies the $v_2(p_T)$ distributions for all three systems onto a single curve for $p_T < 1$ GeV/c. A more intriguing

observation emerges when v_2 is found to scale not with the system's characteristic size - as seen for ε_2 - but with its volume, or more precisely, its volumetric fluctuations (Fig. 6(c)). Here, v_2 is scaled by the product $\varepsilon_2 N_{\rm part}$. This hypothesis is further supported by scaling v_2 with $\varepsilon_2\sigma(\varepsilon_2)^3$ (Fig. 6(d)), which also yields a unified curve. These results suggest that volumetric fluctuations in the initial state might play a significant role in the formation of v_2 and provide a basis for constructing scaling relations to directly compare flow measurements from symmetric and asymmetric collisions. It should be noted, however, that these scaling relations are not stringent, and a more comprehensive investigation – involving models with different implementations of the equation of state of strongly-interacting matter – is required.

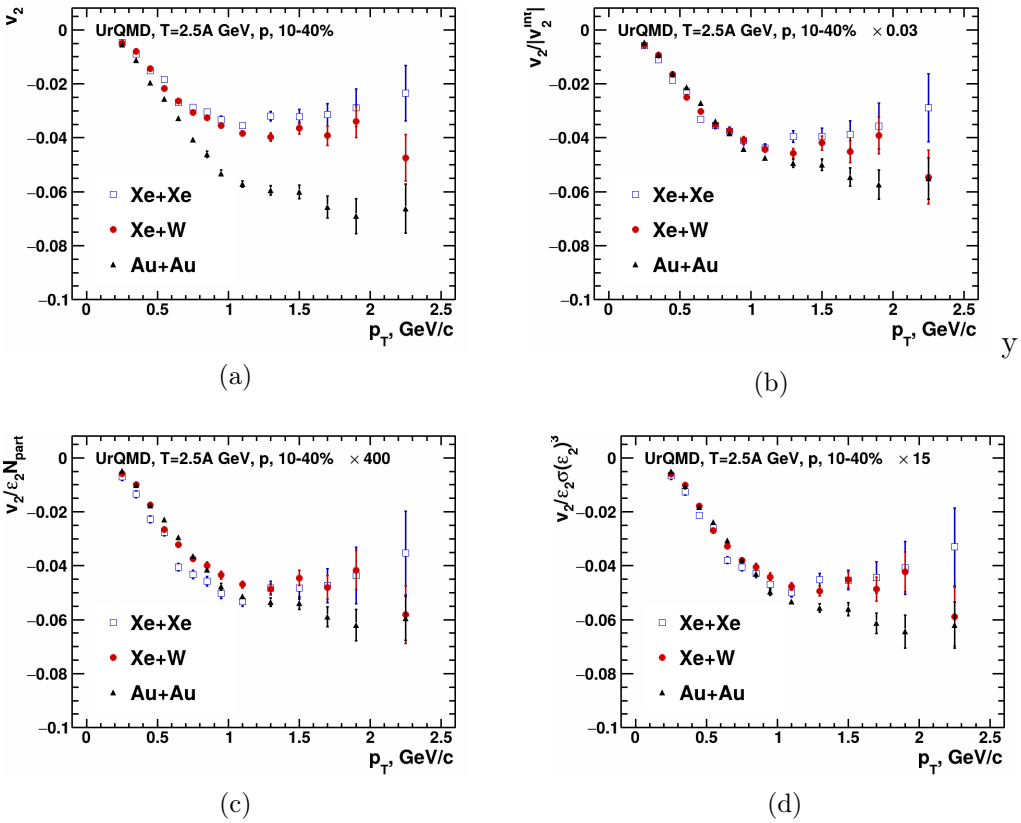


Fig. 6: Proton elliptic flow v_2 as a function of transverse momentum (a), and the corresponding value scaled by the integrated v_2 signal (b), by $\varepsilon_2 N_{\rm part}$ (c), and by $\varepsilon_2\sigma(\varepsilon_2)^3$ (d), from the UrQMD model at a beam kinetic energy of $T = 2.5A$ GeV. Results are shown for mid-central collisions of Xe+Xe (blue), Xe+W (red), and Au+Au (black). For visual clarity, the scaled quantities are multiplied by the factors indicated on each panel.

Conclusions

This work has investigated the initial-state azimuthal anisotropy, characterized by the second-order eccentricity ε_2 and its fluctuations, for the asymmetric Xe+W system relevant to the upcoming MPD-FXT program at NICA. A systematic comparison with symmetric Xe+Xe and Au+Au collisions was performed using both MC-Glauber and UrQMD models at T = 2.5A GeV ($\sqrt{s_{NN}}$ = 2.87 GeV).

We have found that ε_2 scales effectively with the system size when plotted against a scaled impact parameter and multiplicity-based centrality. A key difference emerges in the relative fluctuations $\sigma(\varepsilon_2)$: the MC-Glauber model shows significant system dependence in centralities up to 50-60%, whereas UrQMD predicts similar scaling for both ε_2 and $\sigma(\varepsilon_2)$, highlighting the role of evolution dynamics in the nucleus-nucleus collision.

Furthermore, we demonstrate that the proton elliptic flow v_2 can be unified across symmetric and asymmetric systems by scaling with quantities related to the initial-state volumetric fluctuations – specifically, $\varepsilon_2 N_{\text{part}}$ and $\varepsilon_2\sigma(\varepsilon_2)^3$. This suggests that the initial geometric fluctuations, rather than just the characteristic system size, might play a significant role in the formation of the elliptic flow. These results provide an opportunity to compare flow measurements in asymmetric and symmetric collisions, though further investigation with models implementing different equations of state is needed.

Acknowledgements

The work was funded by the Ministry of Science and Higher Education of the Russian Federation, Project "Studying physical phenomena in the micro- and macro-world to develop future technologies" FSWU-2026-0010.

REFERENCES

1. *Adamczyk L. et al.* [STAR Collaboration] // Phys. Rev. Lett. 2014. V. 112, no. 16. P. 162301.

2. *Adamczyk L. et al.* [STAR Collaboration] // Phys. Rev. Lett. 2018. V. 120, no. 6. P. 062301.

3. *Adamczyk L. et al.* [STAR Collaboration] // Phys. Rev. C. 2013. V. 88. P. 014902.

4. *Adamczyk L. et al.* [STAR Collaboration] // Phys. Rev. C. 2012. V. 86. P. 054908.

5. *Abdallah M.S. et al.* [STAR Collaboration] // Phys. Lett. B. 2022. V. 827. P. 137003.

6. *Kashirin E. et al.* [NA49, NA61/SHINE Collaboration] // Phys. Part. Nucl. 2020. V. 51, no. 3. P. 301–304.

7. *Afanasiev S., others.* // Nucl. Instrum. Meth. A. 2024. V. 1065. P. 169532.
8. *Kekelidze V.D.* // Phys. Part. Nucl. 2018. V. 49, no. 4. P. 457–472.
9. *Abgaryan V. et al.* [MPD Collaboration] // Eur. Phys. J. A. 2022. V. 58, no. 7. P. 140.
10. *Abdulin R. et al.* [MPD Collaboration] // Rev. Mex. Fis. 2025. V. 71, no. 4. P. 041201.
11. *Voloshin S.A., Poskanzer A.M., Snellings R.* // Landolt-Bornstein. 2010. V. 23. P. 293.
12. *Alver B. et al.* [PHOBOS Collaboration] // Phys. Rev. Lett. 2007. V. 98. P. 242302.
13. *Bhalerao R.S., Luzum M., Ollitrault J.Y.* // Phys. Rev. C. 2011. V. 84. P. 054901.
14. *Huang S., Jia J., Zhang C.* // Phys. Lett. B. 2025. V. 870. P. 139926.
15. *Loizides C., Nagle J., Steinberg P.* // SoftwareX. 2015. V. 1-2. P. 13–18.
16. *Bleicher M., others.* // J. Phys. G. 1999. V. 25. P. 1859–1896.
17. *Bass S.A., others.* // Prog. Part. Nucl. Phys. 1998. V. 41. P. 255–369.
18. *Kharzeev D., Nardi M.* // Phys. Lett. B. 2001. V. 507. P. 121–128.
19. *Parfenov P., Troshin V., Taranenko A.* // Phys. Atom. Nucl. 2023. V. 86, no. 6. P. 1493–1497.